THE JOURNAL OF PHYSICAL CHEMISTRY B

Article

pubs.acs.org/JPCB

Noncovalent Interactions in Microsolvated Networks of Trimethylamine *N*-Oxide

Kristina A. Cuellar,[†] Katherine L. Munroe,[‡] David H. Magers,*[,‡] and Nathan I. Hammer*[,†]

[†]Department of Chemistry and Biochemistry, University of Mississippi, P.O. Box 1848, University, Mississippi 38655, United States

[‡]Department of Chemistry and Biochemistry, Mississippi College, P.O. Box 4036, Clinton, Mississippi 39058, United States

Supporting Information

ABSTRACT: The effects of the formation of hydrogen-bonded networks on the important osmolyte trimethylamine N-oxide (TMAO) are explored in a joint Raman spectroscopic and electronic structure theory study. Spectral shifts in the experimental Raman spectra of TMAO and deuterated TMAO microsolvated with water, methanol, ethanol, and ethylene glycol are compared with the results of electronic structure calculations on explicit hydrogen-bonded molecular clusters. Very good agreement between experiment and theory suggests that it is the local hydrogen-bonded geometry at TMAO's oxygen atom that dominates the structure of the extended hydrogen-bonded networks and that TMAO's unique stabilizing abilities are a result of the "indirect effect" model. Natural bonding orbital (NBO) calculations further reveal that hyperconjugation results in vibrational blue shifts in TMAO's C−H stretching region when solvated and a red shift in methanol's C−H stretching region when hydrogen bonding with TMAO.

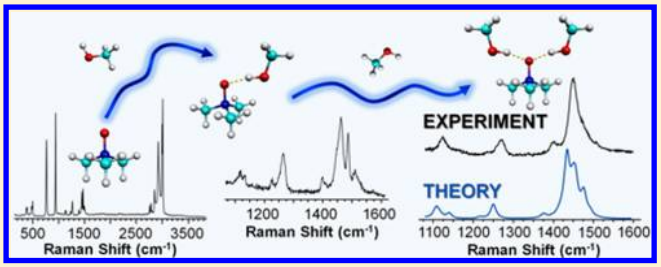

INTRODUCTION

Trimethylamine N-oxide (TMAO) belongs to a class of small biomolecules called osmolytes, which are essential in the biological regulation of water. Some osmolytes, such as urea, are responsible for the denaturating of proteins, whereas TMAO is extremely effective in counteracting this denaturation.[1,2] Despite the importance of osmolytic activity, the exact mechanisms behind osmolyte stabilizing/destabilizing abilities have to date not been fully elucidated. In fact, there persists a controversy as to the molecular origin of the mechanisms being a "direct effect" or "indirect effect".[3−5] A direct effect is one in which the osmolyte directly alters the structure of the protein backbone, whereas an indirect effect is one in which the structure of the solvent is changed by the osmolyte, which in turn changes the structure of the protein.[1,6] Interrogating the effects of noncovalent interactions between osmolytes and their solvents is therefore crucial for understanding and elucidating the mechanism of protection of TMAO.

The large dipole moment of TMAO has been suggested to be an important contributing factor in its ability to stabilize biologically relevant aqueous systems.[7−15] The structure of neighboring water molecules is expected to be affected by such a large dipole moment, supporting the indirect effect mechanism.[8] Researchers have also recently suggested that the main factor behind TMAO's protective behavior is a slowdown of the solvent rotational dynamics.[16,17] Another possible factor leading to the stabilization effect of TMAO may be due to the nature of the N−O bond, which is unique because it can serve as a nucleophile or an oxidant.[18]

TMAO has been reported to strengthen hydrogen bonds in aqueous solutions and is also thought to encourage the creation of more water−water hydrogen bonds with greater spatial ordering.[19] Water also takes on a characteristic ice-like structure when in the vicinity of molecules such as TMAO that possess both hydrophobic and hydrophilic groups.[20] The water molecules preferentially hydrogen bond to the hydrophilic group, which in turn decreases the mobility of the water molecules and leaves a void near the hydrophobic group. The water molecules that are surrounding this void space become essentially immobilized and "ice-like" and do not directly interact with the hydrated molecule.[21,22] This collective phenomenon is commonly referred to as the hydrophobic effect.[20]

We recently elucidated the explicit effects that hydrogen bonded networks of water have on TMAO and showed through good agreement between experiment and theory that each TMAO molecule hydrogen bonds, on average, to three water molecules.[23] Figure 1 shows the structure of TMAO and also the molecular cluster geometry that agreed best with the experimental Raman spectra of aqueous TMAO solutions. We also showed that the water network does not directly interact with the methyl groups to a substantial degree and the best agreement with experiment stemmed from theoretical structures including such a void space.[19] Our previous work suggested that the hydrophobic effect plays a significant role in TMAO's ability to order hydrogen-bonded water networks. We not only studied

Received: August 29, 2013
Revised: December 13, 2013
Published: December 18, 2013

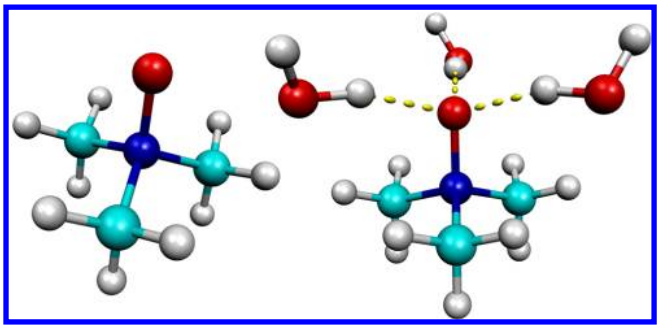

Figure 1. Optimized molecular structure of TMAO (left) as well as TMAO with three water molecules attached (right).[23]

aqueous solutions of TMAO but also monitored time-resolved micro-Raman spectra at the point of microhydration of TMAO in a humid atmosphere. Such measurements at the solid/vapor interface allow for a better description of the intimate intermolecular interactions taking place than can be accomplished by examining bulk solutions of different concentrations. Other recent spectroscopic studies have also showed that water molecules on a hydrophobic surface interact differently − as a separation medium − than when in solution.[24−27]

Our previous study only investigated the special case of TMAO interacting with water. Here we focus on the effects that noncovalent interactions have on TMAO by molecules that cannot form as extensive hydrogen-bonded networks. Such molecules include methanol, ethanol, and ethylene glycol. Both methanol and ethanol are amphoteric and amphiphilic molecules, which contain a hydrophobic group of some hydrocarbon (e.g., CH_3 and CH_2CH_3) as well as a hydrophilic O−H group. Using a custom vacuum chamber, we record the vibrational spectra of TMAO as microsolvation layers are gradually deposited onto TMAO. By tracking the Raman spectra of TMAO from the first step of solvation to fully solvated TMAO, we are able to directly compare the effects of noncovalent interactions with the different solvent molecules.

In addition to interrogating the effects of noncovalent interactions on TMAO, we also explore the effect that TMAO exerts on the solvent molecules. Many previous spectroscopic studies have analyzed the effects of noncovalent interactions on methanol's and ethanol's C−O,[28−30] C−H,[29,31−35] and O−H[28,29] stretching vibrations. For example, Sun et al. demonstrated that ethanol and water vapor behave very differently when interacting with a surface.[36] Whereas ethanol forms a monolayer, water forms a multilayer on the surface due to the fact that water can continually function as a hydrogen-bond donor/acceptor and create an extended hydrogen bonded network while ethanol cannot.[36] Interactions between TMAO and alcohols are of interest because the organic component limits the possibility of hydrogen bond network growth and because it was recently demonstrated that the rotational dynamics of alcohols are slower than that of water due to the lack of the ability to form extended hydrogen-bonded networks.[37] As well as the decreased ability to form hydrogen bonded networks, alcohols also form weaker hydrogen bonds than water,[38] and the hydrogen bonds in ethanol also present a higher degree of thermal stability than those with methanol due to the longer alkyl chain.[39] Venkatesu et al. recently studied the interactions between TMAO and the amphiphilic polymer poly(*N*-isopropylamide) (PNIPAM) in aqueous solution in an attempt to gain insight into the molecular mechanism between protein and TMAO.[40] These authors showed that TMAO weakens hydrogen bonds between the polymer and water, which in turn procures the collapse of the hydrophobic character of the macromolecule.

It has previously been reported both experimentally and theoretically that the O−H groups of water and alcohols exhibit a vibrational red shift (shift to lower frequency) in solution, depending on the concentration of solute.[41−45] Raman spectroscopy was utilized by Onori and Santucci to examine the hydrophobic behavior of TMAO in aqueous solutions.[42] The O−H stretching region (2800−3800 cm^{-1}) of water and the C−H stretching band (2900−3100 cm^{-1}) of TMAO were examined in an attempt to explain the molecular mechanism of protein stabilization/denaturation counteraction by TMAO. The authors noted a small red shift in the O−H stretching region of water and did not see any variations in the C−H stretching region of TMAO. This was the first use of Raman spectroscopy to examine the noncovalent interactions between TMAO and water, which demonstrated that the hydrogen bonds created in solution are stronger than those in the pure solvent itself. In addition, Raman spectra of TMAO have been reported when interacting with various solvents.[46−49] For example, Goubeau and Fromme previously measured the Raman spectra of TMAO in methanol solutions and assigned spectral features to normal modes.[48]

Shifts in vibrational frequencies are helpful in determining the hydrogen-bonding behavior of amphoteric molecules, with red shifts occurring when an alcohol is acting as a proton donor and blue shifts occurring when it is acting as a proton acceptor when properly hydrogen-bonded.[50] For example, in 2009, Keefe et al. performed a Raman and FTIR spectroscopic study and showed that the C−H stretching region of methanol exhibits a blue shift with decreasing methanol mole fraction when interacting with either acetonitrile or water in binary mixtures, indicating that improper hydrogen bonding is plausible.[51] Later, Keefe and Istvankova studied changes in vibrational frequencies of the O−H, C−H, and C−O vibrations of methanol involved in proper and improper hydrogen bonds.[52] They concluded that when methanol is acting as hydrogen-bond donor, the O−H and C−H bands are red-shifted if properly hydrogen-bonded, and the C−H region blue shifts if improperly hydrogen-bonded.

When water molecules hydrogen bond to the hydroxyl group of the alcohol and the structure of bulk water is conserved, this has been referred to as "incomplete mixing" at the molecular level.[53] This hydrophobic segregation suggests that at low methanol concentrations in aqueous solution the methanol molecules orient their methyl groups away from the water layer, and this is accompanied by the loss in entropy of the solution as opposed to the increase in entropy that occurs with ideal solutions.[54] In fact, the hydrophilic and hydrophobic forces of alcohols play a large role in its solvation structure and dynamics.[55] In our previous study, however, we showed that microhydration of TMAO resulted in the most dramatic changes in its Raman spectra and that there are no further spectroscopic effects with bulk dilution once TMAO is initially solvated.[23] This result suggests that the oxygen atom on TMAO may dominate the extended hydrogen-bonded network.[56]

Spectral shifts in the Raman vibrational spectra of TMAO when microsolvated with water, methanol, ethanol, and ethylene glycol allow us here to explore the effects that different hydrogen-bonded networks have on TMAO. By obtaining time-resolved Raman spectra of TMAO in the presence of these vapor-phase hydrogen-bond donors, we are able to observe the effects of gradual microsolvation by these molecules on TMAO.[57] Comparison of the experimental shifts in the Raman spectra of

dx.doi.org/10.1021/jp408659n | *J. Phys. Chem. B* 2014, 118, 449−459

TMAO[14,47,58−60] when microsolvated to theoretical predictions allows for a molecular-level description of these hydrogen bonded interactions.

EXPERIMENTAL SECTION

Spectroscopic Methods. Commercial-grade anhydrous trimethylamine N-oxide (Sigma-Aldrich), D9-trimethylamine N-oxide (Cambridge Isotope Laboratories), methanol (Fisher-Scientific), ethanol (Pharmco-AAPER), ethylene glycol (Fisher-Scientific), and D4-methanol (Cambridge Isotope Laboratories, 99.8%) were used without further purification. The excitation source employed for Raman spectroscopy was the 514.5 nm line from a Coherent Innova 200 Ar ion laser. The spectra were collected using a Jobin-Yvon Ramanor HG2-S Raman spectrometer with two 1800 grooves/mm gratings and a thermoelectrically cooled (−30 °C) photomultiplier tube detector. A scan speed of 2 cm^{-1}/s was employed for spectra shown. Spectra were obtained for the solid state of TMAO in a vacuum chamber, and time-resolved spectra of solid TMAO in the presence of vapor-phase solvent were obtained to qualitatively show the effects of microsolvation of neat TMAO. A vacuum chamber, which connects to a liquid reservoir and vacuum, was developed and is shown in Figure 2. The chamber

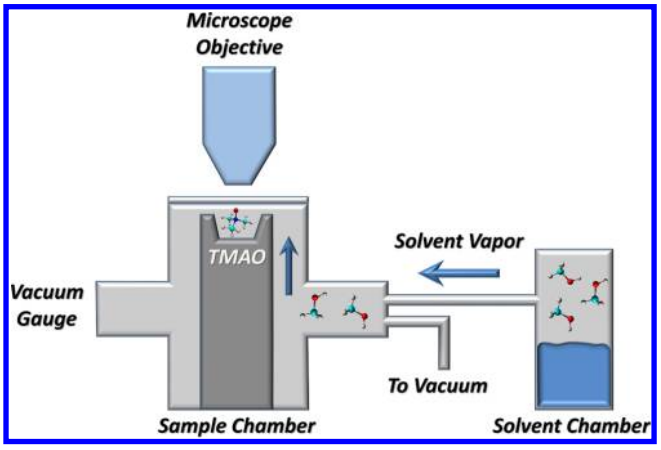

Figure 2. Custom Raman spectroscopy setup. Solvent vapor is introduced to solid-phase TMAO in vacuum.

allows for the analysis of TMAO and D9-TMAO and other solid-phase samples in an atmosphere of the experimenter's choice. In this case, a series of hydrogen-bond donors including water, methanol, ethanol, and ethylene glycol were employed in the studies of microsolvation of neat TMAO.

Theoretical Methods. Geometry optimizations and frequency calculations were performed on a 16-core Quantum Cube from Parallel Quantum Solutions using the *PQS* ab initio program package version 3.314.[61] Optimum equilibrium geometries and corresponding electronic energies of TMAO and TMAO with methanol, ethanol, and ethylene glycol molecules were determined using density functional theory.[62,63] The B3LYP hybrid functional comprising Becke's three-parameter functional[64] using the LYP correlation functional of Lee, Yang, and Parr[65] with the augmented correlation consistent basis set aug-cc-pVTZ by Dunning and coworkers was utilized.[66,67] The vibrational frequencies of pure TMAO, D9-TMAO, methanol, D4-methanol, and TMAO with two methanol molecules were also calculated anharmonically using the *Gaussian 09* software package[68] with the MP2 method and the aug-cc-pVTZ and aug-cc-pVDZ basis sets to aid in the assignment of fundamentals and combination bands in TMAO's and methanol's C−H stretching region. Natural bond orbital (NBO) calculations were performed on TMAO, methanol, and select molecular clusters using the *Gaussian 09* software package[68] using the B3LYP method and aug-cc-pVTZ basis set. Simulated spectra were constructed with a custom program developed with National Instruments *LabView*.

SPECTROSCOPIC RESULTS

TMAO is a very hygroscopic molecule and quickly forms a thin layer of water in a humid atmosphere.[23] In fact, many previous vibrational spectroscopic investigations involving TMAO were complicated by this phenomenon. Here spectra were acquired in a specially designed vacuum chamber in the presence of water, methanol, ethanol, and ethylene glycol vapor. Shown in Figures 3−6 are Raman spectra of TMAO in the presence of increasing

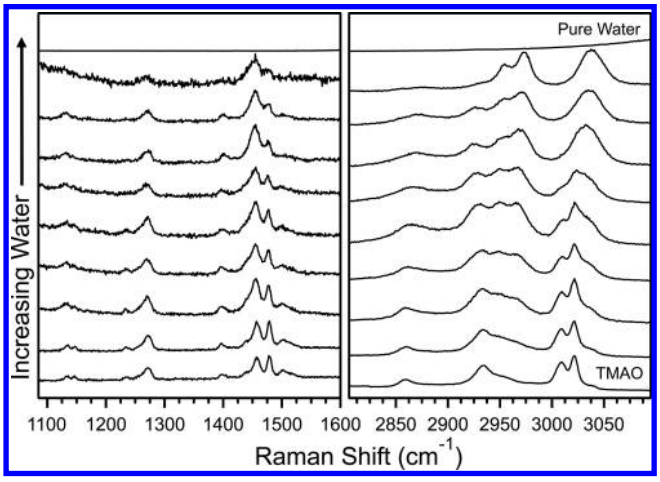

Figure 3. Raman spectra of TMAO during microsolvation with water. The bottom spectrum is anhydrous TMAO in vacuum.

amounts of water, methanol, ethanol, and ethylene glycol, respectively. Raman spectra of pure liquid water, methanol, ethanol, and ethylene glycol are included for comparison.

In the C−H stretching region of anhydrous TMAO (shown in Figure 3), there are three sets of peaks that evolve with increasing

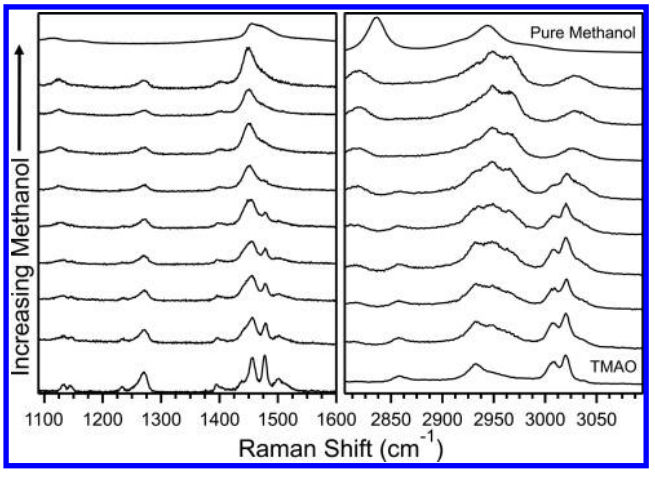

Figure 4. Raman spectra of TMAO during microsolvation with methanol compared with the spectrum of pure methanol.

dx.doi.org/10.1021/jp408659n | J. Phys. Chem. B 2014, 118, 449−459

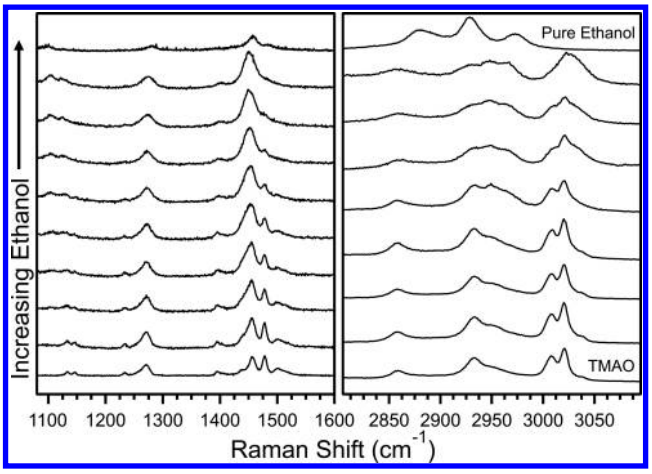

Figure 5. Raman spectra of TMAO during microsolvation with ethanol compared with the spectrum of pure ethanol.

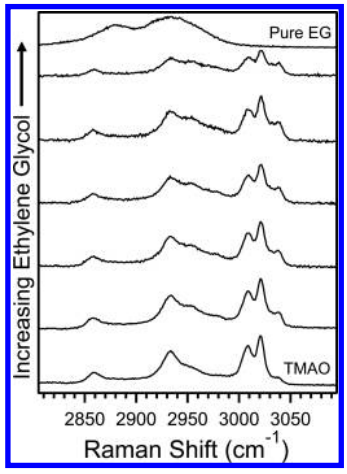

Figure 6. Raman spectra of TMAO during microsolvation with ethylene glycol (EG) compared with the spectrum of pure ethylene glycol.

hydration. The highest energy doublet residing at just greater than 3000 cm^{-1} in anhydrous TMAO slowly converges into a broad single feature that is blue-shifted in comparison with the original doublet. This final peak at 3030 cm^{-1} is the highest intensity peak in this region and corresponds to asymmetric C−H stretching of TMAO's methyl groups. A small peak at ∼3038 cm^{-1} steadily emerges with hydration and merges into this feature. The emergence of this new peak at 3038 cm^{-1} is the spectral signature of solvation.[23] The second set of peaks of interest in the C−H stretching region involve a prominent peak at 2930 cm^{-1} and two overlapped peaks starting at ∼2955 cm^{-1}. These are symmetric C−H stretching modes of TMAO. With hydration, the prominent peak at 2930 cm^{-1} decreases in intensity and red shifts to lower energy as the overlapped peaks increase in intensity, separate, and blue shift to final spectral positions at 2962 and 2974 cm^{-1}. The unassigned peak at 2860 cm^{-1} in anhydrous TMAO slowly broadens and slightly blue shifts with hydration. The C−H bending region of TMAO is characterized by three sets of peaks that correspond to different linear combinations of C−H bending motions of TMAO's three methyl groups. The prominent doublet at 1455 and 1479 cm^{-1} increasingly red shift and collapses into one feature at 1450 cm^{-1}. A nearby small peak at 1500 cm^{-1} also disappears with solvation. Interestingly, the peak 1270 cm^{-1} only decreases slightly in intensity but does not shift. The small doublet between 1125 and 1150 cm^{-1} gradually red shifts and collapses into one feature at 1130 cm^{-1}.

The spectra of TMAO when microsolvated by methanol, ethanol, and ethylene glycol exhibit many similarities to those of TMAO microhydrated with water. Both the C−H stretching and bending regions of TMAO are similarly affected by all three alcohols. The overall structure of TMAO becomes less pronounced as more solvent is deposited, with the two main doublets at approximately 1450 and 3000 cm^{-1} becoming single features, as in the case of water. Additional Raman features of all three alcohols themselves also contribute to the overall Raman spectra. There are some noticeable differences, however, between TMAO's spectrum hydrated with water and solvated with the three organic molecules, especially in the C−H stretching region. In the case of methanol microsolvation (Figure 4), a peak at 2815 cm^{-1} attributed to methanol slowly enters and intensifies with increasing microsolvation. Also, the peak at 2860 cm^{-1} blue shifts when hydrated but does not shift with methanol, ethanol, or ethylene glycol deposition. Unfortunately, there are many possible overtones and combination bands that can account for this peak. In the C−H bending region, all of the features behave similarly with microsolvation.

THEORETICAL RESULTS

Shown in Figures 7−9 are optimized molecular structures of TMAO/methanol, TMAO/ethanol, and TMAO/ethylene glycol clusters as well as their corresponding simulated Raman spectra. In each case, one or more alcohol molecules hydrogen bond to TMAO's oxygen atom. Table 1 shows the energies of each of the clusters as well as their relative energies to each other. The Table, as well as each of the simulated spectra, is ordered with increasing number of alcohol molecules attached to TMAO and increasing relative energy. In the case of methanol (Figure 7), structures with two hydrogen bonds to the oxygen atom of TMAO generally are more stable, although this is not the case with 4M-A, which has three hydrogen bonds and is 2.01 kcal/mol lower in energy than 4M-B, which has two hydrogen bonds to oxygen. The opposite is true in the case of ethanol and ethylene glycol, however. In ethanol, structures with one hydrogen bond to the oxygen atom of TMAO tend to be more stable than those with two hydrogen bonds. Structure 1E-C is much higher in energy than other structures due to the fact that instead of ethanol hydrogen bonding with the oxygen on TMAO, TMAO is hydrogen bonding to the oxygen in ethanol via TMAO's methyl groups. Interestingly, in ethylene glycol, structures with the fewest number of hydrogen bonds to TMAO's oxygen atom are the most stable.

DEUTERATED SPECTROSCOPIC AND ANHARMONIC THEORETICAL RESULTS

Because of overlap of spectral features upon microsolvation, especially in the C−H stretching region, the microsolvation spectra of TMAO with D4-methanol and also D9-TMAO with H4-methanol were acquired and are shown in Figures 10 and 11, respectively. In addition, anharmonic frequency calculations on methanol, D4-methanol, TMAO, and D9-TMAO were performed and compared with experimental Raman spectra to aid in the assignment of normal modes in these molecules. These results are shown in Figure 12. Table 2 lists a number of predicted combination bands and overtones that could account for the additional peaks in the experimental C−H and C−D stretching spectra.

dx.doi.org/10.1021/jp408659n | J. Phys. Chem. B 2014, 118, 449−459

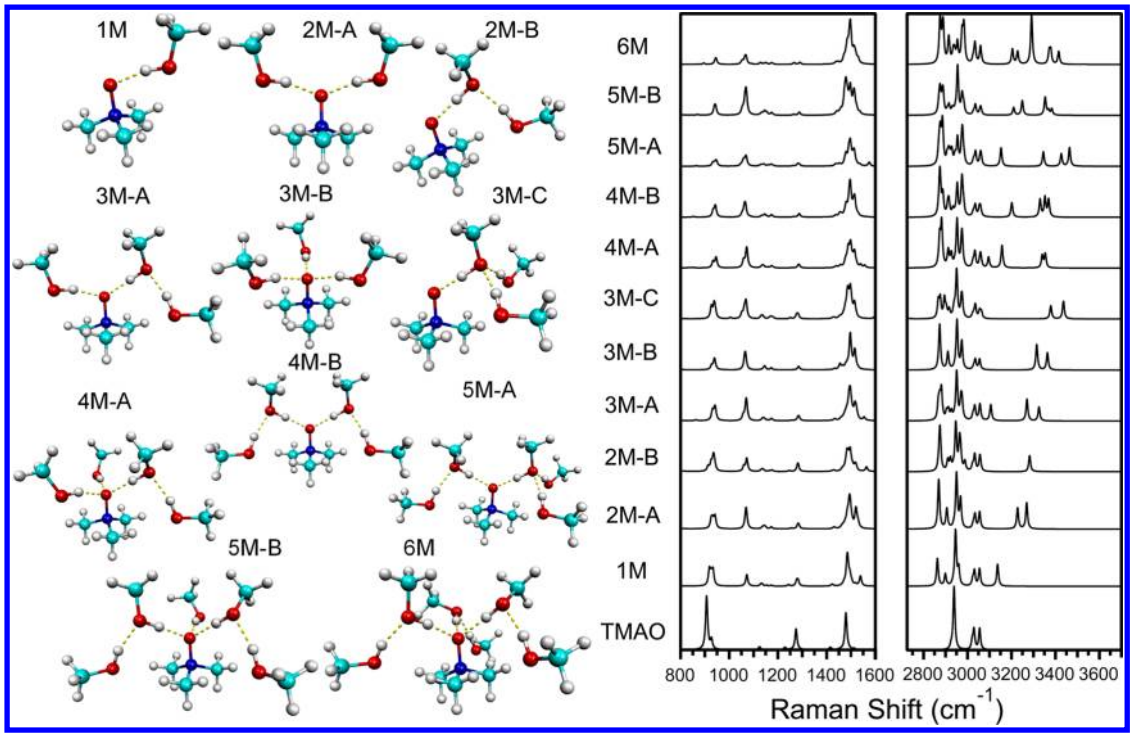

Figure 7. Optimized structures of TMAO with 1 to 6 methanol molecules as well as the corresponding simulated Raman spectra compared with an isolated TMAO molecule.

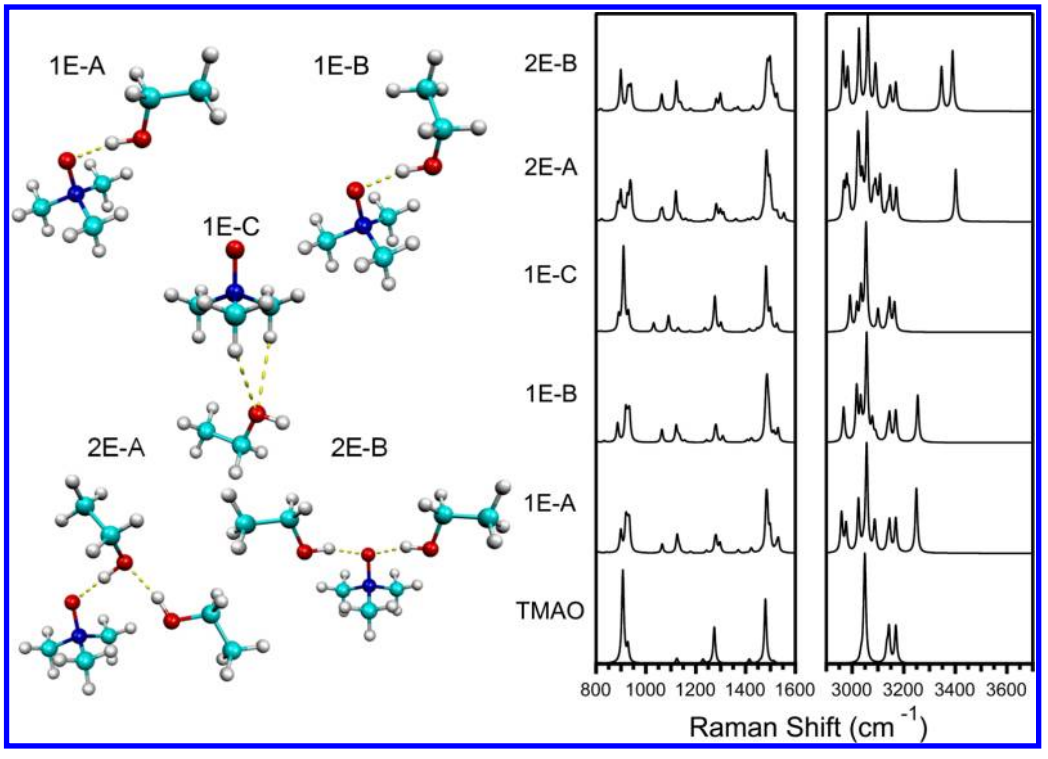

Figure 8. Optimized structures of TMAO with one or two ethanol molecules as well as the corresponding simulated Raman spectra compared with an isolated TMAO molecule.

NATURAL BONDING ORBITALS (NBO) RESULTS

Tables 3 and 4 list the changes in NBO populations (in me^-)[70,71] for methanol and TMAO in the 2M-A structure and water and TMAO for our previously reported 3W−B structure, respectively, relative to the individual noninteracting molecules. The largest change in the case of methanol comes in methanol's O−H σ^* orbital, which gains 42 me^- per methanol molecule, and at the same time, TMAO's oxygen lone pairs and C−N σ^* orbitals lose electron density. Methanol's C−H σ^* orbitals also exhibit a slight increase in electron population. A similar effect is observed in the case of water where 35 me^- are gained by each water's O−H σ^*

dx.doi.org/10.1021/jp408659n | J. Phys. Chem. B 2014, 118, 449−459

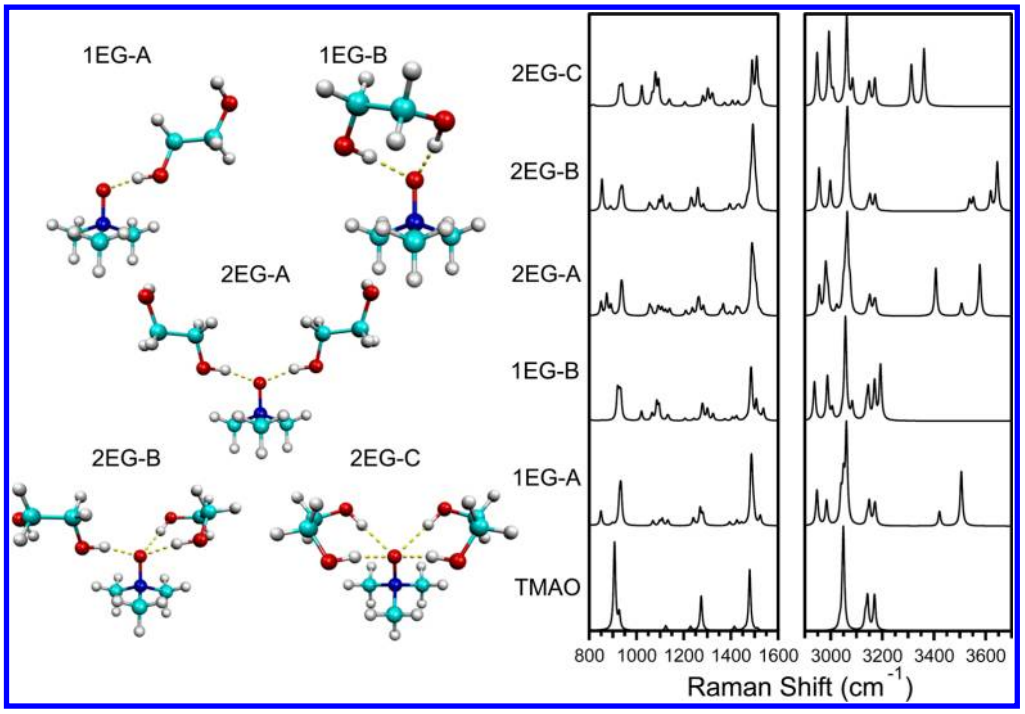

Figure 9. Optimized structures of TMAO with one or two ethylene glycol molecules as well as the corresponding simulated Raman spectra compared with an isolated TMAO molecule.

Table 1. Computed Energies, Zero Point Energies, and Relative Energies for TMAO and Microsolvated Clusters

structure	energy (au)	zero point energy (au)	ZPE corrected (au)	relative energy (kcal/mol)
TMAO	−249.72179	0.125	−249.59679	
1M	−365.52520	0.178	−365.34720	
2M-A	−481.30944	0.232	−481.07744	0.00
2M-B	−481.30301	0.232	−481.07101	4.04
3M-A	−597.09922	0.285	−596.81422	0.00
3M-B	−597.09821	0.285	−596.81321	0.63
3M-C	−597.09351	0.284	−596.80951	2.95
4M-A	−712.89306	0.338	−712.55506	0.00
4M-B	−712.88985	0.338	−712.55185	2.01
5M-A	−828.68207	0.391	−828.29107	0.00
5M-B	−828.68202	0.391	−828.29102	0.03
6M	−944.47290	0.444	−944.02890	
1E-A	−404.84602	0.206	−404.64002	0.00
1E-B	−404.84698	0.207	−404.63998	0.02
1E-C	−404.82784	0.205	−404.62284	10.80
2E-A	−559.97671	0.288	−559.68871	0.00
2E-B	−559.97531	0.288	−559.68731	0.88
1EG-A	−480.10155	0.213	−479.88855	0.00
1EG-B	−480.09242	0.211	−479.88142	4.48
2EG-A	−710.46789	0.300	−710.16789	0.00
2EG-B	−710.46600	0.301	−710.16500	1.81
2EG-C	−710.46030	0.298	−710.16230	3.51

orbital. The net effect in the 3W-B structure[23] is larger due to the presence of three water molecules.

DISCUSSION

Spectral shifts in the experimental microsolvated Raman spectra of TMAO interacting with the hydrogen bond donors methanol, ethanol, and ethylene glycol are very similar to those observed with water. This result suggests that interactions with TMAO's oxygen atom are dominating the local solvation geometry. Raman spectra of TMAO solvated with deuterated methanol (see Figure 11) allow for a direct comparison of the effects of solvation on TMAO's C−H stretching modes between water and methanol without spectral overlap with the C−H stretches of methanol. We previously showed that the emergence of a new peak at 3038 cm^{-1} is the spectral signature of hydration of TMAO.[23] This feature is common to Raman spectra of TMAO solvated with all of the hydrogen-bond donors studied here. In the comparison in Figure 11 of TMAO solvated with water and methanol, this peak is much more intense in the case of water. At the same time, the two overlapped peaks starting at 2955 cm^{-1} that increase in intensity, separate, and blue shift to final spectral positions of 2962 and 2974 cm^{-1} in water also exhibit a different ratio in the case of methanol. These features stem from asymmetric C−H stretching motions in solvated TMAO, and their blue-shifted positions are recovered by the theoretical results. The higher intensities of these blue-shifted features in the TMAO fully solvated with water suggest a stronger interaction than in the case of methanol.

The striking similarities in the Raman spectra of TMAO solvated with water and the solvents studied here suggest a common structural motif in all of the hydrogen-bonded complexes. We previously showed that in the case of hydrogen bonding with water a symmetric complex with three water molecules hydrogen-bonded to TMAO's oxygen atom (see Figure 1) yielded excellent agreement between experiment and theory. When TMAO is microsolvated by methanol, the lowest energy and more stable theoretical structures tend to correspond to TMAO molecules, which are hydrogen-bonded to two methanol molecules. This is not the case with TMAO microsolvated by ethanol. In this case, the lowest energy structure that was identified exhibits bonding between TMAO and only one ethanol molecule, with the second ethanol molecule preferring to hydrogen bond to the first ethanol

dx.doi.org/10.1021/jp408659n | J. Phys. Chem. B 2014, 118, 449−459

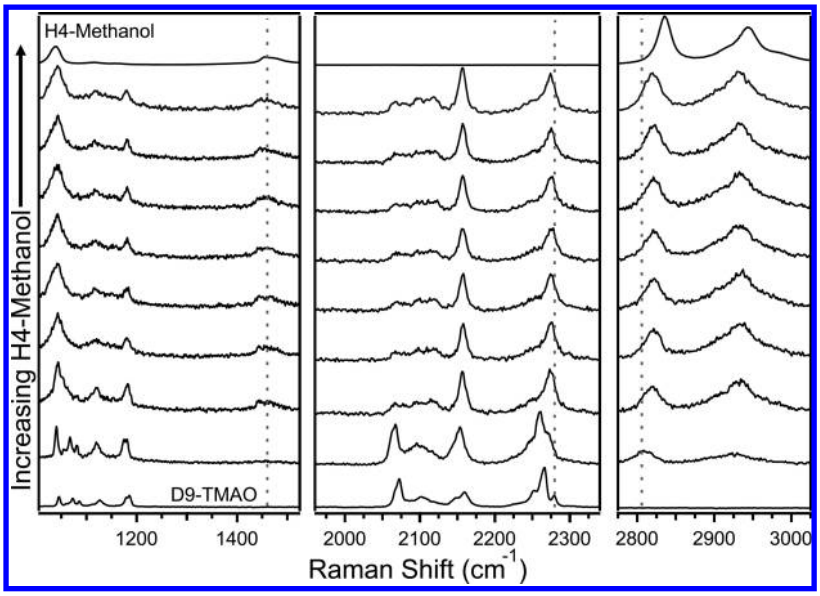

Figure 10. Raman spectra of solid anhydrous D9-TMAO during microsolvation with H4-methanol compared with the spectrum of pure methanol. The bottom spectrum is D9-TMAO in air. The appearance of the small feature at 2280 cm^{-1} indicates slight exposure to water vapor prior to study.

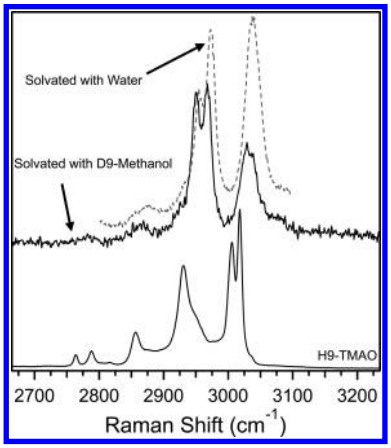

Figure 11. Raman spectra of solid anhydrous H9-TMAO compared with TMAO solvated with D4-methanol (solid curve) and water (dotted curve).

molecule rather than TMAO. This difference in stability could stem from the fact that the size of ethanol is twice that of methanol so that more methanol molecules are able to interact with TMAO.[72]

The best agreement between experiment and theory in the case of TMAO solvated with methanol comes from structures having their methyl groups oriented away from TMAO's methyl groups and the hydrogen bonds between the O−H groups of the alcohol and the oxygen on TMAO. Two such structures are the theoretical structures 2M-A and 3M-B. This is the same situation as we observed previously with water, where TMAO was shown to hydrogen bond to three water molecules.[23] With ethanol, the theoretical structures in best agreement with experiment are the 1E-A and 1E-B structures with one ethanol molecule. These two structures are very close in energy with the 1E-A structure being slightly more stable. This structure orients the methyl groups of both the TMAO and the ethanol closer together than the 1E-B structure, which has the methyl groups oriented away from each other.

In the spectrum of TMAO and methanol, there is a methanol peak in the stretching region (2825 cm^{-1}) that is red-shifted in comparison with pure methanol. This is shown in Figure 9 and suggests that hydrogen bonding with TMAO is affecting methanol's hydrogen-bonded network relative to liquid-phase methanol. The fact that this peak red shifts confirms that methanol is acting as a hydrogen bond donor and is bonding to TMAO via the hydroxyl hydrogen.[50,52] The results of the NBO analysis on structure 2M-A reveal that the oxygen atom on TMAO experiences a decrease in electron population, while the O−H σ^* orbital of methanol experiences an almost equal but opposite increase in electron population upon complex formation. At the same time, there are small changes in methanol's C−H σ and σ^* orbital populations. One C−H bond in methanol is a different length than the other two and increases in electron population in the σ orbital as well as the σ^* orbital but to a lesser degree than the other C−H antibonding orbitals. The other two methyl bonds decrease in electron population in their σ bonding orbitals but increase in charge in the σ^* orbitals. In addition to charge rearrangement, all three C−H bonds as well as the O−C bond in methanol elongate. The elongation of these bonds, as well as the increase in electron population of the σ^* orbitals, is likely the origin of the observed experimental red shift of the C−H stretching mode at 2825 cm^{-1}. This hyperconjugation leads to a direct correlation between the charge transfer, change in bond distance, and observed shifts of vibrational modes.[71,73,74] A similar hyperconjugative effect is also observed in TMAO, where one of the C−H bond lengths and orbital populations differs from the other two in each methyl group. This charge transfer is likely the origin of the blue shifting of TMAO's C−H stretching peaks.[23,74] The results of an NBO analysis on our previously reported 3W-B structure[23] reveal a similar effect in the case of water. Just as in the case of methanol, the C−H bonds in TMAO do not respond equally. However, the net transfer in the case of water is larger and is likely the origin of the greater blue shift and ratio of peaks observed in Figure 11.

The C−H (and C−D) stretching region of alcohols is complicated due to overlapping symmetric and asymmetric C−H stretching vibrations, Fermi resonances, and C−H bending overtones.[31,75] In methanol, the lower frequency peak (2830

dx.doi.org/10.1021/jp408659n | J. Phys. Chem. B 2014, 118, 449−459

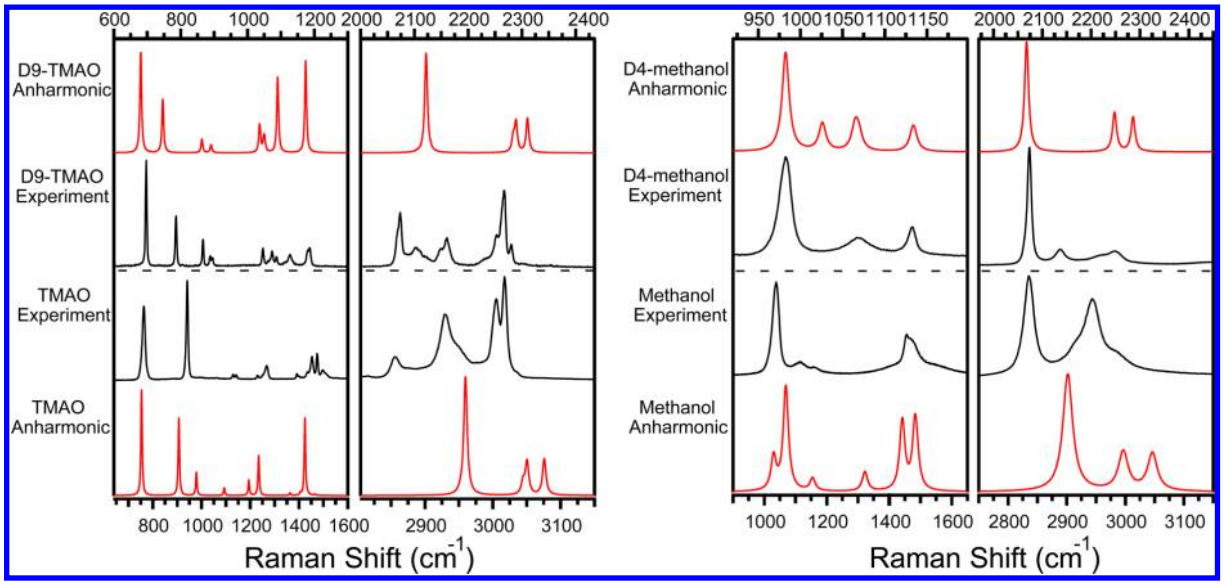

Figure 12. Comparison of the experimental (black) Raman spectra of TMAO and D9-TMAO (left) and methanol and D4-methanol (right) with the simulated (red) results of anharmonic frequency calculations.

Table 2. Possible Overtone and Combination Bands Predicted by Anharmonic Calculations Performed at the MP2/aug-cc-pVTZ Level to Aid in the Assignment of the Experimental Mode at 2860 cm^{-1} in TMAO's Spectra (left), C-D Stretching Modes of D4-Methanol (center), and C−H stretching Modes of H4-methanol (right)

mode(s) TMAO[23]	frequency (cm^{-1})	mode(s) MeOD[69]	frequency (cm^{-1})	mode(s) MeOH[69]	frequency (cm^{-1})
3	2937	10	2144	3	2849
16	2882	6	2127	5 + 10	2806
17	2842	4	2064	7 + 3	2914
4 + 3	2873	6 + 4	2202	7 + 10	2800
16 + 3	2908	10 + 4	2198	3 + 5	2923
17 + 3	2889	10 + 6	2127		
16 +16	2885	5 + 4	2161		

cm^{-1}) has previously been attributed to the fundamental symmetric stretch[33,75−77] or a Fermi resonance[29,78,79] composed of a stretching fundamental and a bending overtone. The assignment of the second peak in methanol's C−H stretching region is also under debate, being attributed to either the asymmetric stretch[33,80−82] or the previously described Fermi resonance. A recent study suggested that the two peaks at 2830 and 2950 cm^{-1} are involved in a Fermi resonance of the symmetric ν_3 mode and a bending overtone or combination band. The lower frequency peak was suggested to consist of a mixture of the ν_3 symmetric stretch, the ν_5 symmetric deformation, and two asymmetric deformations, ν_4 and ν_{10}, while the higher frequency peak consists of a mixture of the ν_3 symmetric stretch and the ν_5 symmetric deformation.[31] The anharmonic results presented here in Table 2 and Figure 12 suggest that the C−H stretching region does likely contain overtones and combination bands involving modes that correspond to bending motions of the C−H bonds. However, the excellent agreement shown in Figure 12 between the C−D bending and stretching spectra of D-4 methanol and the

Table 3. Population Changes (in me^-) of the B3LYP/aug-cc-pVTZ NBOs of Methanol and TMAO from the 2M-A Structure Relative to the Noninteracting Molecules

methanol			TMAO				
orbital		Δq (me^-)	orbital		Δq (me^-)	orbital	Δq (me^-)
σ	(O1 H2)	−2	σ	(O1 N2)	−2	n (O1)	−24
σ	(O1 C3)	0	σ	(N2 C3)	0	σ* (O1 N2)	7
σ	(C3 H4)	−1	σ	(N2 C7)	0	σ* (N2 C3)	−11
σ	(C3 H5)	1	σ	(N2 C11)	0	σ* (N2 C7)	−9
σ	(C3 H6)	−1	σ	(C3 H4)	−1	σ* (N2 C11)	−11
n	(O1)	−6	σ	(C3 H5)	−1	σ* (C3 H4)	0
n	(O1)	−8	σ	(C3 H6)	−2	σ* (C3 H5)	1
σ*	(O1 H2)	42	σ	(C7 H8)	−1	σ* (C3 H6)	−3
σ*	(O1 C3)	2	σ	(C7 H9)	−2	σ* (C7 H8)	1
σ*	(C3 H4)	2	σ	(C7 H10)	−1	σ* (C7 H9)	−3
σ*	(C3 H5)	1	σ	(C11 H12)	−2	σ* (C7 H10)	1
σ*	(C3 H6)	2	σ	(C11 H13)	−1	σ* (C11 H12)	−3
			σ	(C11 H14)	−1	σ* (C11 H13)	1
			n	(O1)	−11	σ* (C11 H14)	0
			n	(O1)	3		

dx.doi.org/10.1021/jp408659n | J. Phys. Chem. B 2014, 118, 449−459

Table 4. Population Changes (in me$^-$) of the B3LYP/aug-cc-pVTZ NBOs of Water and TMAO from the 3W-B[23] Structure Relative to the Non-Interacting Molecules

water			TMAO					
orbital		Δq (me$^-$)	orbital		Δq (me$^-$)	orbital		Δq (me$^-$)
σ	(H1 O2)	−2	σ	(O1 N2)	−2	n	(O1)	−7
σ	(O2 H3)	−1	σ	(N2 C3)	0	σ^*	(O1 N2)	11
n	(O2)	−1	σ	(N2 C7)	0	σ^*	(N2 C3)	−13
n	(O2)	−3	σ	(N2 C11)	0	σ^*	(N2 C7)	−13
σ^*	(H1 O2)	35	σ	(C3 H4)	−1	σ^*	(N2 C11)	−13
σ^*	(O2 H3)	1	σ	(C3 H5)	−1	σ^*	(C3 H4)	0
			σ	(C3 H6)	−3	σ^*	(C3 H5)	1
			σ	(C7 H8)	−1	σ^*	(C3 H6)	−4
			σ	(C7 H9)	−3	σ^*	(C7 H8)	0
			σ	(C7 H10)	−1	σ^*	(C7 H9)	−4
			σ	(C11 H12)	−3	σ^*	(C7 H10)	1
			σ	(C11 H13)	−1	σ^*	(C11 H12)	−4
			σ	(C11 H14)	−1	σ^*	(C11 H13)	0
			n	(O1)	−18	σ^*	(C11 H14)	1
			n	(O1)	−7			

anharmonic fundamental results suggests that an overtone of the asymmetric deformation likely accounts for the appearance of the peak at 2133 cm^{-1} and that the other three fundamentals are mostly pure symmetric and asymmetric stretches. Taking this into account, the poor agreement between the experimental H4-methanol C−H stretching spectra and the anharmonic fundamental simulated spectrum suggests the peak at 2830 is participating in a Fermi resonance, likely with the overtone of the asymmetric deformation.

Figure 13 shows a comparison of the TMAO's Raman C−H bending spectrum when microsolvated with methanol to a simulated anharmonic vibrational spectrum performed at the MP2/aug-cc-PVDZ level on the 2M-A structure. The excellent agreement strongly suggests that TMAO is, on average, bonding to two methanol molecules. Anharmonic vibrational frequency calculations performed on the 2M-A structure for the C−H stretching region also confirm the red shift experimentally observed for methanol when hydrogen bonded to TMAO. Experimentally, the red shift for methanol's symmetric stretch is 18 cm^{-1}, whereas the anharmonic calculation predicts a red shift of 21 cm^{-1}. Interestingly, one spectral feature in the Raman spectrum of TMAO that does not behave the same upon solvation is the feature at 2860 cm^{-1} in the C−H stretching region. This feature blue shifts and broadens when TMAO is microhydrated by water, but this is not the case with the alcohol solvents. The peak does not exhibit a shift when the solvent employed is methanol, ethanol, or ethylene glycol. The results of the anharmonic calculations (Table 2) suggest that a number of different overtones or combination bands could account for this peak, and the nature of this mode may explain the different behavior observed for water and alcohols. A definitive assignment of this mode, however, remains elusive.

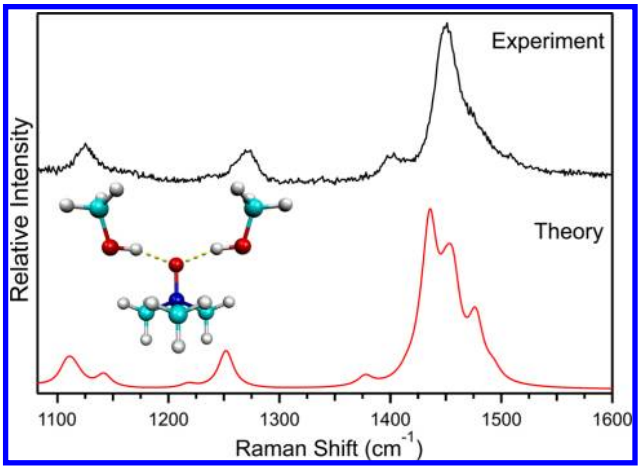

Figure 13. Comparison of the experimental (black) Raman spectra of the 2M-A structure to the simulated (red) result from an anharmonic frequency calculation in the C−H bending region.

CONCLUSIONS

The similarities in the Raman spectra of microsolvated TMAO using a variety of hydrogen bond donors suggest a common structural motif in all of the hydrogen-bonded complexes. In particular, the arrangement of hydrogen bonds with TMAO's oxygen atom appears to dictate the extended hydrogen-bonded network and is likely the origin of TMAO's osmolytic strength via the indirect effect. Hyperconjugation is observed in both TMAO and the hydrogen-bonded solvent molecules. This charge transfer leads to blue shifts in TMAO's C−H stretching modes and a dramatic red shift in methanol's symmetric stretch. The effect is larger in the case of water and is likely the origin of TMAO's blue-shifted C−H stretching modes in solution.

ASSOCIATED CONTENT

Supporting Information

Cartesian coordinates of the optimized clusters on the TMAO molecule. This material is available free of charge via the Internet at http://pubs.acs.org.

AUTHOR INFORMATION

Corresponding Authors

*D.H.M.: E-mail: magers@mc.edu.
*N.I.H.: E-mail: nhammer@olemiss.edu.

Notes

The authors declare no competing financial interest.

■ ACKNOWLEDGMENTS

This work has been partially supported by the National Science Foundation (EPS-0903787 and CHE-0955550). We wish to thank Prof. Gregory S. Tschumper for helpful discussions.

■ REFERENCES

(1) Bolen, D. W.; Rose, G. D. Structure and Energetics of the Hydrogen-Bonded Backbone in Protein Folding. *Annu. Rev. Biochem.* **2008**, *77*, 339−362.
(2) Zhang, Y. J.; Cremer, P. S. Chemistry of Hofmeister Anions and Osmolytes. *Annu. Rev. Phys. Chem.* **2010**, *61*, 63−83.
(3) Attri, P.; Venkatesu, P.; Lee, M.-J. Influence of Osmolytes and Denaturants on the Structure and Enzyme Activity of A-Chymotrypsin. *J. Phys. Chem. B* **2010**, *114*, 1471−1478.
(4) Canchi, D. R.; García, A. E. Cosolvent Effects on Protein Stability. *Annu. Rev. Phys. Chem.* **2013**, *64*, 273−293.
(5) Kuffel, A. The Hydrogen Bond Network Structure within the Hydration Shell around Simple Osmolytes: Urea, Tetramethylurea, and Trimethylamine-N-Oxide, Investigated Using Both a Fixed Charge and a Polarizable Water Model. *J. Chem. Phys.* **2010**, *133*, 035102−035109.
(6) Wei, H.; Fan, Y.; Gao, Y. Q. Effects of Urea, Tetramethyl Urea, and Trimethylamine N-Oxide on Aqueous Solution Structure and Solvation of Protein Backbones: A Molecular Dynamics Simulation Study. *J. Phys. Chem. B* **2010**, *114*, 557−568.
(7) Kocherbitov, V.; Veryazov, V.; Soderman, O. Hydration of Trimethylamine-N-oxide and of Dimethyldodecylamine-N-oxide: An Ab Initio Study. *J. Mol. Struct. (THEOCHEM)* **2007**, *808*, 111−118.
(8) Maclagan, R.; Malardier-Jugroot, C.; Whitehead, M. A.; Lever, M. Theoretical Studies of the Interaction of Water with Compensatory and Noncompensatory Solutes for Proteins. *J. Phys. Chem. A* **2004**, *108*, 2514−2519.
(9) Linton, E. P. The Dipole Moments of Amine Oxides. *J. Am. Chem. Soc.* **1940**, *62*, 1945−1948.
(10) Armstrong, R. S.; Aroney, M. J.; Calderbank, K. E.; Pierens, R. K. Molar Kerr Constants and Solute Polarizability Anisotropies of Ammonia, Trimethylamine, Trimethylamine Oxide and 1,4-Diazabicyclo[2.2.2]Octane. *Aust. J. Chem.* **1977**, *30*, 1411−1415.
(11) Phillips, G. M.; Hunter, J. S.; Sutton, L. E. An Investigation of the Occurrence of the Co-Ordinate or Dative Link by Electric Dipole-Moment Measurements. *J. Chem. Soc.* **1945**, 146−162.
(12) Tsygankova, N. G.; Bubel, O. N.; Grinshpan, D. D.; Kaputskii, F. N. Mndo Calculation of Steric and Electronic Structure of Molecules of Tertiary Amine Oxides. *Vestsi Akad. Navuk BSSR, Ser. Khim. Navuk* **1988**, 35−37.
(13) Yakimanskii, A. V.; Bochek, A. M.; Zubkov, V. A.; Petropavlovskii, G. A. Quantum-Chemical Analysis of the Electronic Structure of Solvents for Cellulose (Amine Oxides). *Zh. Prikl. Khim.* **1991**, *64*, 622−626.
(14) Kast, K. M.; Brickmann, J.; Kast, S. M.; Berry, R. S. Binary Phases of Aliphatic N-Oxides and Water: Force Field Development and Molecular Dynamics Simulation. *J. Phys. Chem. A* **2003**, *107*, 5342−5351.
(15) Kast, K. M.; Reiling, S.; Brickmann, J. Ab Initio Investigations of Hydrogen Bonding in Aliphatic N-Oxide-Water Systems. *J. Mol. Struct. (THEOCHEM)* **1998**, *453*, 169−180.
(16) Saladino, G. A Simple Mechanism Underlying the Effect of Protecting Osmolytes on Protein Folding. *J. Chem. Theory Comput.* **2011**, *7*, 3846−3852.
(17) Hunger, J. Complex Formation in Aqueous Trimethylamine-N-Oxide (TMAO) Solutions. *J. Phys. Chem. B* **2012**, *116*, 4783−4795.
(18) Rogachev, A. Y. Bonding Situation and No-Bond Strengths in Amine-N-Oxides–a Combined Experimental and Theoretical Study. *Phys. Chem. Chem. Phys.* **2012**, *14*, 1985−2000.
(19) Zou, Q.; Bennion, B. J.; Daggett, V.; Murphy, K. P. The Molecular Mechanism of Stabilization of Proteins by Tmao and Its Ability to Counteract the Effects of Urea. *J. Am. Chem. Soc.* **2002**, *124*, 1192−1202.
(20) Tanford, C. *The Hydrophobic Effect*; Wiley: New York, 1980.
(21) Frank, H. S. S. Free Volume and Entropy in Condensed Systems III. Entropy in Binary Liquid Mixtures; Partial Molal Entropy in Dilute Solutions; Structure and Thermodynamics in Aqueous Electrolytes. *J. Chem. Phys.* **1945**, *13*, 507−533.
(22) Rezus, Y. L. A.; Bakker, H. J. Observation of Immobilized Water Molecules around Hydrophobic Groups. *Phys. Rev. Lett.* **2007**, *99*, 148301−148304.
(23) Munroe, K. L.; Magers, D.; Hammer, N. I. Raman Spectroscopic Signatures of Noncovalent Interactions between Trimethylamine N-Oxide (TMAO) and Water. *J. Phys. Chem. B* **2011**, *115*, 7699−7707.
(24) Shibukawa, M.; Kondo, Y.; Ogiyama, Y.; Osuga, K.; Saito, S. Interfacial Water on Hydrophobic Surfaces Recognized by Ions and Molecules. *Phys. Chem. Chem. Phys.* **2011**, *13*, 15925−15935.
(25) Scatena, L. F.; Brown, M. G.; Richmond, G. L. Water at Hydrophobic Surfaces: Weak Hydrogen Bonding and Strong Orientation Effects. *Science* **2001**, *292*, 908−912.
(26) Tarbuck, T. L.; Ota, S. T.; Richmond, G. L. Spectroscopic Studies of Solvated Hydrogen and Hydroxide Ions at Aqueous Surfaces. *J. Am. Chem. Soc.* **2006**, *128*, 14519−14527.
(27) Gopalakrishnan, S.; Liu, D.; Allen, H. C.; Kuo, M.; Shultz, M. J. Vibrational Spectroscopic Studies of Aqueous Interfaces: Salts, Acids, Bases, and Nanodrops. *Chem. Rev.* **2006**, *37*, 1155−1175.
(28) Rai, D. Methanol Clusters (Ch3oh)N, N = 3−6 in External Electric Fields: Density Functional Theory Approach. *J. Chem. Phys.* **2011**, *135*, 024307−024319.
(29) Ebukuro, T. Raman Spectroscopic Studies on Hydrogen Bonding in Methanol and Methanol/Water Mixtures under High Temperature and Pressure. *J. Supercrit. Fluids* **1999**, *15*, 73−78.
(30) Ahmed, M. K. The C-O Stretching Infrared Band as a Probe of Hydrogen Bonding in Ethanol-Water and Methanol-Water Mixtures. *Spectrosc. Lett.* **2012**, *45*, 420−423.
(31) Ishiyama, T.; Sokolov, V. V.; Morita, A. Molecular Dynamics Simulation of Liquid Methanol. II. Unified Assignment of Infrared, Raman, and Sum Frequency Generation Vibrational Spectra in Methyl C-H Stretching Region. *J. Chem. Phys.* **2011**, *134*, 024510−024520.
(32) Colles, M. J.; Griffiths, J. E. Relative and Absolute Raman Scattering Cross Sections in Liquids. *J. Chem. Phys.* **1972**, *56*, 3384−3391.
(33) Kamogawa, K.; Kitagawa, T. Solute/Solvent and Solvent/Solvent Interactions in Methanol Solutions: Quantitative Separation by Raman Difference Spectroscopy. *J. Phys. Chem.* **1985**, *89*, 1531−1537.
(34) Zhu, X.; Yao, J.; Li, H.; Han, S. Prediction among Different Spectroscopic Properties for Aqueous Systems. *J. Chem. Phys.* **2006**, *124*, 244501−244505.
(35) Kamogawa, K.; Kaminaka, S.; Kitagawa, T. Behavior of Ethanol in Various Binary Solutions: Difference Raman Spectroscopy on the C-H Stretching Vibrations. *J. Phys. Chem.* **1987**, *91*, 222−226.
(36) Cheng, T.; Sun, H. Adsorption of Ethanol Vapor on Mica Surface under Different Relative Humidities: A Molecular Simulation Study. *J. Phys. Chem. C* **2012**, 16436−16446.
(37) Vartia, A. A. On the Reorientation and Hydrogen-Bond Dynamics of Alcohols. *J. Phys. Chem. B* **2011**, *115*, 12173−12178.
(38) Shao, Q. From Protein Denaturant to Protectant: Comparative Molecular Dynamics Study of Alcohol/Protein Interactions. *J. Chem. Phys.* **2012**, *136*, 115101−115109.
(39) Miura, Y. Nmr Studies on Thermal Stability of A-Helix Conformation of Melittin in Pure Ethanol and Ethanol-Water Mixture Solvents. *J. Pept. Sci.* **2011**, *17*, 798−804.
(40) Reddy, P. M.; Taha, M.; Venkatesu, P.; Kumar, A.; Lee, M. J. Destruction of Hydrogen Bonds of Poly(N-Isopropylacrylamide) Aqueous Solution by Trimethylamine N-Oxide. *J. Chem. Phys.* **2012**, *136*, 234904−234913.
(41) Fileti, E. E. Calculated Infrared Spectra of Hydrogen-Bonded Methanol-Water, Water-Methanol, and Methanol-Methanol Complexes. *Int. J. Quantum Chem.* **2005**, *104*, 808−815.
(42) Di Michele, A.; Freda, M.; Onori, G.; Paolantoni, M.; Santucci, A.; Sassi, P. Modulation of Hydrophobic Effect by Cosolutes. *J. Phys. Chem. B* **2006**, *110*, 21077−21085.

(43) Freda, M.; Onori, G.; Santucci, A. Infrared and Dielectric Spectroscopy Study of the Water Perturbation Induced by Two Small Organic Solutes. *J. Mol. Struct.* **2001**, *565*−*566*, 153−157.
(44) Freda, M.; Onori, G.; Santucci, A. Infrared Study of the Hydrophobic Hydration and Hydrophobic Interactions in Aqueous Solutions of Tert-Butyl Alcohol and Trimethylamine-N-Oxide. *J. Phys. Chem. B* **2001**, *105*, 12714−12718.
(45) Freda, M.; Onori, G.; Santucci, A. Hydrophobic Hydration and Hydrophobic Interaction in Aqueous Solutions of Tert-Butyl Alcohol and Trimethylamine-N-Oxide: A Correlation with the Effect of These Two Solutes on the Micellization Process. *Phys. Chem. Chem. Phys.* **2002**, *4*, 4979−4984.
(46) Kahovec, L. The Raman Spectrum of Trimethylamine Oxide. *Anz. Akad. Wiss. Wien, Math.-Naturwiss. Kl.* **1944**, *81*, 32−34.
(47) Kuroda, Y.; Kimura, M. Vibrational Spectra of Trimethylamine Oxide Dihydrate. *Spectrochim. Acta* **1966**, *22*, 47−56.
(48) Goubeau, J.; Fromme, I.; Nitrogen-Oxygen Bond, I. Nitrogen-Oxygen Bonds without Mesomerism. *Z. Anorg. Chem.* **1949**, *258*, 18−26.
(49) Edsall, J. T. Raman Spectra of Amino Acids and Related Substances III. Ionization and Methylation of the Amino Group. *J. Chem. Phys.* **1937**, *5*, 225−237.
(50) Karpfen, A. Blue-Shifted A-H Stretching Frequencies in Complexes with Methanol: The Decisive Role of Intramolecular Coupling. *Phys. Chem. Chem. Phys.* **2011**, *13*, 14194−14201.
(51) Keefe, C. D.; Gillis, E. A. L.; MacDonald, L. Improper Hydrogen-Bonding Ch·Y Interactions in Binary Methanol Systems as Studied by Ftir and Raman Spectroscopy. *J. Phys. Chem. A* **2009**, *113*, 2544−2550.
(52) Keefe, C. D.; Istvankova, Z. Computational Study of Proper and Improper Hydrogen Bonding in Methanol Complexes. *Can. J. Chem.* **2011**, *89*, 34−46.
(53) Dixit, S.; Crain, J.; Poon, W. C. K.; Finney, J. L.; Soper, A. K. Molecular Segregation Observed in a Concentrated Alcohol-Water Solution. *Nature* **2002**, *416*, 829−832.
(54) Pascal, T. A.; Goddard, W. A. Hydrophobic Segregation, Phase Transitions and the Anomalous Thermodynamics of Water/Methanol Mixtures. *J. Phys. Chem. B* **2012**, *116*, 13905−13912.
(55) Ghosh, M. K.; Uddin, N.; Choi, C. H. Hydrophobic and Hydrophilic Associations of a Methanol Pair in Aqueous Solution. *J. Phys. Chem. B* **2012**, *116*, 14254−14260.
(56) Rösgen, J.; Jackson-Atogi, R. Volume Exclusion and H-Bonding Dominate the Thermodynamics and Solvation of Trimethylamine-N-Oxide in Aqueous Urea. *J. Am. Chem. Soc.* **2012**, *134*, 3590−3597.
(57) Baber, A. E.; Lawton, T. J.; Sykes, E. C. H. Hydrogen-Bonded Networks in Surface-Bound Methanol. *J. Phys. Chem. C* **2011**, *115*, 9157−9163.
(58) Choplin, F.; Kaufmann, G. Vibration Spectra and Normal Coordinate Analysis of Trimethylamine, Trimethylphosphine, and Trimethylarsine Oxides. *Spectrochim. Acta, Part A* **1970**, *26*, 2113−2124.
(59) Giguere, P. A.; Chin, D. An Infrared Study of Trimethylamine Oxide, Its Hydrate, and Its Hydrochloride. *Can. J. Chem.* **1961**, *39*, 1214−1220.
(60) Mathis, R. Absorption Spectra of Some Tertiary Amine Oxides. *C. R. Chim.* **1956**, *242*, 1873−1876.
(61) Pulay, P.; Baker, J.; Wolinski, K. *PQS Ab Initio Program Package*; Parallel Quantum Solutions: Fayetteville, AR, 2007.
(62) Hohenberg, P. Inhomogeneous Electron Gas. *Phys. Rev.* **1964**, *136*, B864−B871.
(63) Kohn, W. Self-Consistent Equations Including Exchange and Correlation Effects. *Phys. Rev.* **1965**, *140*, A1133−A1138.
(64) Becke, A. D. Density-Functional Thermochemistry. III. The Role of Exact Exchange. *J. Chem. Phys.* **1993**, *98*, 5648−5652.
(65) Lee, C. Development of the Colle-Salvetti Correlation-Energy Formula into a Functional of the Electron Density. *Phys. Rev. B: Condens. Matter Mater. Phys.* **1988**, *37*, 785−789.
(66) Dunning, T. H., Jr. Gaussian Basis Sets for Use in Correlated Molecular Calculations. I. The Atoms Boron through Neon and Hydrogen. *J. Chem. Phys.* **1989**, *90*, 1007−1023.
(67) Kendall, R. A. Electron Affinities of the First-Row Atoms Revisited. Systematic Basis Sets and Wave Functions. *J. Chem. Phys.* **1992**, *96*, 6796−6806.
(68) Frisch, M.; Trucks, G.; Cheeseman, J.; Scalmani, G.; Clemente, F.; Caricato, M.; Patel, P.; Fox, D.; Morokuma, K.; Jacokowski, I., et al. *Gaussian*, revision A.1; Gaussian, Inc.: Wallingford, CT, 2009.
(69) Ishiyama, T.; Sokolov, V. V.; Morita, A. Molecular Dynamics Simulation of Liquid Methanol. I. Molecular Modeling Including C-H Vibration and Fermi Resonance. *J. Chem. Phys.* **2011**, *134*, 024509−024526.
(70) Howard, A. A.; Tschumper, G. S.; Hammer, N. I. Effects of Hydrogen Bonding on Vibrational Normal Modes of Pyrimidine. *J. Phys. Chem. A* **2010**, *114*, 6803−6810.
(71) Wright, A. M.; Howard, A. A.; Howard, J. C.; Tschumper, G. S.; Hammer, N. I. Charge Transfer and Blue Shifting of Vibrational Frequencies in a Hydrogen Bond Acceptor. *J. Phys. Chem. A* **2013**, *117*, 5435−5446.
(72) Siler, A. R.; Walker, R. A. Effects of Solvent Structure on Interfacial Polarity at Strongly Associating Silica/Alcohol Interfaces. *J. Phys. Chem. C* **2011**, *115*, 9637−9643.
(73) Chandra, A. K.; Parveen, S.; Zeegers-Huyskens, T. Anomeric Effects in the Symmetrical and Asymmetrical Structures of Triethylamine. Blue-Shifts of the C−H Stretching Vibrations in Complexed and Protonated Triethylamine. *J. Phys. Chem. A* **2007**, *111*, 8884−8891.
(74) Chandra, A. K.; Parveen, S.; Das, S.; Zeegers-Huyskens, T. Blue Shifts of the C–H Stretching Vibrations in Hydrogen-Bonded and Protonated Trimethylamine. Effect of Hyperconjugation on Bond Properties. *J. Comput. Chem.* **2008**, *29*, 1490−1496.
(75) Stanners, C. D.; Du, Q.; Chin, R. P.; Cremer, P.; Somorjai, G. A.; Shen, Y. R. Polar Ordering at the Liquid-Vapor Interface of N-Alcohols (C1-C8). *Chem. Phys. Lett.* **1995**, *232*, 407−413.
(76) Ma, G.; Allen, H. C. Surface Studies of Aqueous Methanol Solutions by Vibrational Broad Bandwidth Sum Frequency Generation Spectroscopy. *J. Phys. Chem. B* **2003**, *107*, 6343−6349.
(77) Schwartz, M.; Moradi-Araghi, A.; Koehler, W. H. Fermi Resonance in Aqueous Methanol. *J. Mol. Struct.* **1980**, *63*, 279−285.
(78) Devendorf, G. S.; Hu, M.-H. A.; Ben-Amotz, D. Pressure Dependent Vibrational Fermi Resonance in Liquid CH_3OH and CH_2Cl_2. *J. Phys. Chem. A* **1998**, *102*, 10614−10619.
(79) Arencibia, A.; Taravillo, M.; Caceres, M.; Nunez, J.; Baonza, V. G. Pressure Tuning of the Fermi Resonance in Liquid Methanol: Implications for the Analysis of High-Pressure Vibrational Spectroscopy Experiments. *J. Chem. Phys.* **2005**, *123*, 214502−214510.
(80) Iwaki, L. K.; Dlott, D. D. Ultrafast Vibrational Energy Redistribution within C−H and O−H Stretching Modes of Liquid Methanol. *Chem. Phys. Lett.* **2000**, *321*, 419−425.
(81) Pogorelov, V.; Bulavin, L.; Doroshenko, I.; Fesjun, O.; Veretennikov, O. The Structure of Liquid Alcohols and the Temperature Dependence of Vibrational Bandwidth. *J. Mol. Struct.* **2004**, *708*, 61−65.
(82) Wang, C.-y.; Groenzin, H.; Shultz, M. J. Surface Characterization of Nanoscale Tio2 Film by Sum Frequency Generation Using Methanol as a Molecular Probe. *J. Phys. Chem. B* **2003**, *108*, 265−272.